Emerging extreme value and Fermi-Dirac distributions in the Lévy branching and annihilating process

F. C. dos Anjos, M. L. Lyra, and Iram Gléria
Instituto de Física, Universidade Federal de Alagoas, 57072-970 Maceió-AL, Brazil

C. Argolo
Instituto Federal de Ciência e Tecnologia do Estado de Alagoas, 57020-510 Maceió-AL, Brazil and Núcleo de Ciências Exatas - NCEx, Universidade Federal de Alagoas, 57309-005 Arapiraca-AL, Brazil

Adauto J. F. de Souza
Departamento de Física, Universidade Federal Rural de Pernambuco, 52171-900 Recife-PE, Brazil

(Received 13 January 2020; revised manuscript received 20 March 2020; accepted 6 May 2020; published 26 May 2020)

We study the dynamics of the branching and annihilating process with long-range interactions. Static particles generate an offspring and annihilate upon contact. The branching distance is supposed to follow a Lévy-like power-law distribution with $P(r) \propto 1/r^{\alpha}$. We analyze the long term behavior of the mean particles number and its fluctuations as a function of the parameter α that controls the range of the branching process. We show that the dynamic exponent associated with the particle number fluctuations varies continuously for $\alpha < 4$ while the particle number exponent only changes for $\alpha < 3$. A crossover from extreme value Frechet (at $\alpha = 3$) and Gumbell (for $2 < \alpha < 3$) distributions is developed, similar to the one reported in recent experiments with cw-pumped random fiber lasers presenting underlying gain and Lévy processes. We report the dependence of the relevant dynamical power-law exponents on α showing that explosive growth takes place for $\alpha \leqslant 2$. Further, the average occupation number distribution is shown to evolve from the standard Fermi-Dirac form to the generalized one within the context of nonextensive statistics.

DOI: 10.1103/PhysRevE.101.052136

I. INTRODUCTION

Branching and annihilating processes represent an important class of nonequilibrium dynamical systems finding applications in several branches of science, including condensed matter, statistical physics, physical chemistry, biology, ecology, and sociology [1–12]. In these processes, particles can generate offspring while annihilating upon contact. When the particles execute a random walk in a lattice, the competition between particle generation through branching and particle destruction through annihilation may lead to the extinction of the population depending on the relative strength of these competing processes. When branching predominates, the system evolves to a statistically stationary state with a finite density of particles. On the other hand, extinction is the dynamical attractor at low branching rates.

The above phenomenology is usually termed as an absorbing state nonequilibrium phase transition between an active and a vacuum state [13,14]. This transition has a close analogy with the standard second-order phase transition associated with a spontaneous breaking of symmetry in condensed matter systems at thermal equilibrium with a heat bath. Critical exponents characterize the universality class of these nonequilibrium phase transitions. The most common is the directed percolation universality class [13–16]. This is actually the case of the absorbing state phase transition of branching and annihilation random walkers with an odd number of offspring [17–21]. However, a new universality class is in order when the branching process conserves the parity of the particle number (even number of offspring) [17,22–25].

Long-range processes are also able to change the universality class of nonequilibrium phase transitions [6,26–30]. These processes can be introduced in the dynamical rules by considering the particle diffusion to be anomalous with the distance r of individual jumps on the lattice following a Lévy-like distribution $P(r) \propto 1/r^{\alpha}$. Here, α governs the effective range of the long-ranged process. It has been demonstrated that the critical exponents of the absorbing state phase transition changes continuously as a function of α below a threshold value. The long-range process can be also introduced in the own branching process while keeping normal diffusion, also leading to continuously varying exponents [6,30].

In the pure branching and annihilation process, particles are not allowed to diffuse [31–34]. In this case, although branching and annihilation are competing processes, the average number of particles grows in time when the system starts from a single particle seed. For the case of a single offspring such growth is linear, while a slower diffusive behavior takes place when two offsprings are placed symmetrically on the neighboring sites of a one-dimensional lattice [5]. However, the influence of long-range interactions in the dynamics of the pure branching and annihilation process is still an open issue.

In this work we will address the above question by studying the dynamics of the pure Lévy branching and annihilation process in a one-dimensional lattice. In particular, we will be interested in determining the time evolution of the particle number and its fluctuations. These usually develop power-law growth when the system starts from a single seed particle. The characteristic dynamic exponents of these two relevant quantities will be estimated from numerical simulations in the entire range of values for the Lévy exponent α. We will unveil the associated distribution functions, exploring the regimes of Gaussian and non-Gaussian fluctuations as well as the emergence of extreme value distributions. A crossover from Frechet (at threshold) to Gumbell extreme values distributions will be reported. This result closely resembles recent experimental findings on cw-pumped random fiber laser [35]. Further, the average occupation number distribution functions in distinct branching regimes will be explored.

II. THE PURE LEVY BRANCHING AND ANNIHILATION PROCESS

Here, we consider the branching and annihilating of *static* particles A that generate a single offspring $A \rightarrow 2A$ to the left or to the right with equal probability. The particles annihilate upon contact $A + A \rightarrow \oslash$, i.e., when the branching process tries to generate an offspring in an already occupied site. These processes can be represented by the reaction equations

$$A \longrightarrow (nA + A), \tag{1}$$

$$A + A \longrightarrow \oslash. \tag{2}$$

Here, $n = 1$ is the number of offspring. The branching distance r is assumed to follow a Lévy power-law distribution. This is effectively accounted by choosing the branching distance as

$$r = (1 - x)^{-1/(\alpha-1)}. \tag{3}$$

Here, x is a uniformly distributed random number in the interval $0 \leqslant x < 1$. Only the integer part of r is considered. It follows a Lévy power-law distribution in the form

$$P(r) \propto \frac{1}{r^{\alpha}} \tag{4}$$

with α controlling the ranging of the branching process. Large values of α correspond to short range interactions (offspring generated in the close vicinity of the parental particle). Conversely, small values of α allows for large branching distances r.

The model is simulated in a one dimensional lattice of size L. The lattice size L was chosen to be close to the largest integer supported by our hardware. In all runs, the total time evolution was chosen to avoid finite size effects, avoiding the process to reach the chain borders. At each elementary step, one particle of the system is chosen at random to generate an offspring. Time is increased by $1/N(t)$ at each step, where $N(t)$ is the number of particles at time t. Configurational averages are taken over a large number of independent runs. As the time elapses, the mean number of particles in the lattice grows without limit. Due to the absence of diffusion, an absorbing state in which the population vanishes cannot be reached, even with no parity conservation.

Here, we study the long term behavior of the mean number of particles $\overline{N}(t)$. We start from the initial condition with a single particle in the center of a one dimensional lattice. We also followed the time evolution of the quadratic fluctuations in the particle number defined as

$$\Delta N^2(t) = \overline{[N(t) - \overline{N}(t)]^2}. \tag{5}$$

In our simulations the mean number $\overline{N}(t)$ and its fluctuations are calculated over a large number of samples, specified in the next section. Power-law behaviors are expected at sufficiently large times:

$$\overline{N}(t) \sim t^{\theta}, \tag{6}$$

$$\Delta N^2(t) \sim t^{\phi} \tag{7}$$

with θ being the dynamic exponent associated with the growth of the average particle number and ϕ the corresponding one associated with its fluctuations. For short-range branching, it is well known that the average number of particles grows linearly in time ($\theta = 1$) presenting Gaussian fluctuations ($\phi = 1$) [5]. Our goal is to analyze how the above quantities vary in time for distinct α values, i.e., how long-range branching affects the dynamic exponents. We are mainly interested in α outside the regime $0 < \alpha < 2$. In fact, in those cases very large jumps are often observed. Mutual annihilation becomes rare thus rendering the mean number of particles to diverge exponentially in time.

III. RESULTS

We start our analysis by showing a space-time plot in distinct branching regimes. Figure 1 shows the spatial distribution of particles, over time, for some representative α values. The simulations were performed in a one-dimensional (1D) lattice. Data are shown up to $t = 300$. In all cases, the initial condition is one single particle in the center of the lattice. In Fig. 1(a) we have $\alpha = 2.5$. The particles spread over a wide region of the lattice because a small α corresponds to an effective long-range branching. New seeds appear throughout the lattice due to branching to an empty region. The low population density around the neighborhood of the new generated particle leads to few encounters and therefore few extinctions. In this way, particles quickly spread over the lattice. Figure 1(b) shows the results for $\alpha = 3$. The particles do not spread over very large distances and kept concentrated around a small region surrounding the center of the lattice. Short-ranged branching makes the offspring to be usually generated in an already occupied site, leading to extinction of both particles. Note that, for large values of t, some offspring may be generated in sites far from the original central position, as expected since the distance r follows a power law distribution whose fat tails guarantee the occurrence of outlier events. Figure 1(c) considers $\alpha = 3.5$. The particles are aggregated in a even smaller region around the origin since faraway branching are less likely, a similar situation presented in Fig. 1(d), which considers $\alpha = 4$. For these values of α most of the offspring are generated around

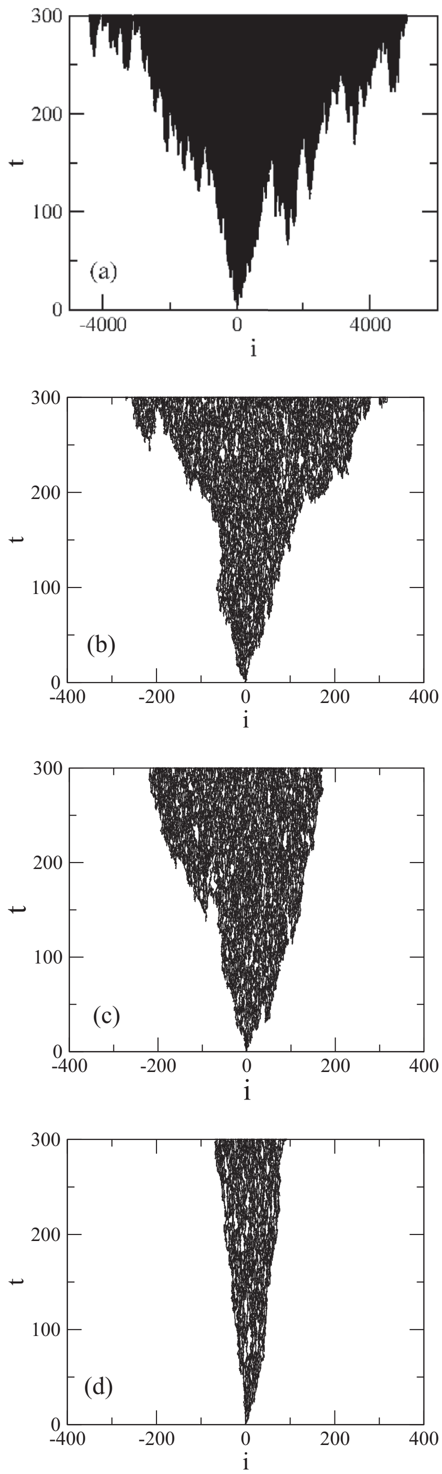

FIG. 1. Space-time distribution of particles for distinct α values. In (a) $\alpha = 2.5$, (b) $\alpha = 3.0$, (c) $\alpha = 3.5$, and (d) $\alpha = 4.5$. For small α, there are long-range branchings to unoccupied regions of the chain which favors a fast occupation of the lattice. For large α, short-range branching predominates and the population growth is slower. Notice the distinct spacial scale in (a) which hides the small gaps of unoccupied sites evident in (b)–(d).

the central initial position and the annihilation mechanism forbids a high occupation rate. The spacial distribution of particles over time is thus connected to the value of α that

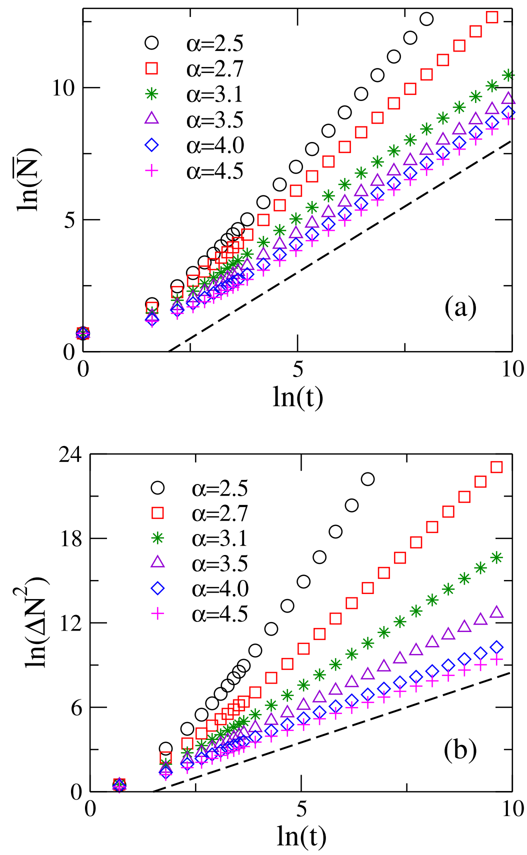

FIG. 2. In (a) we present the time evolution of the mean number of particles, and in (b) its quadratic fluctuations for distinct values of α. The long-time slopes give the respective dynamic exponents. Notice that, while the dynamic exponent of $\overline{N}(t)$ starts to change for $\alpha < 3$, its fluctuation exponent already deviates from the short-range behavior for $\alpha < 4$. Dashed lines have unitary slope corresponding to the expected short-range behavior.

furnishes the typical size r of the branching distance. Small α favors branching to empty regions, leading to a faster population growth. For large values of α, there is (almost) no occurrence of large jumps and it is likely for an offspring to be created in an already occupied site, leading to a slower population increase.

Since the value of α, which controls the branching distance, governs the range of the interactions, we now focus on the dynamical exponents related to the average number of particles and its fluctuations. In Fig. 2 we have the time evolution of the mean number of particles and its fluctuations for a wide range of α values. We checked that no attempt to branch outside the chain borders occurred during any time run. As such, our results are free from finite-size corrections. The number of samples varied from 10^4 for the smallest α to 10^5 for the largest ones. For $\alpha < 3$ we stopped the simulations after $t = 5000$ (otherwise finite-size effects would affect the simulations). For $\alpha > 3$ we run up to $t = 50000$ with no finite-size effect due to the shorter-range character of the branching process.

Figure 2(a) shows the log-log time evolution of the mean number of particles. The results show that, for $\alpha < 3$, the mean number of particles grows faster as the α value is

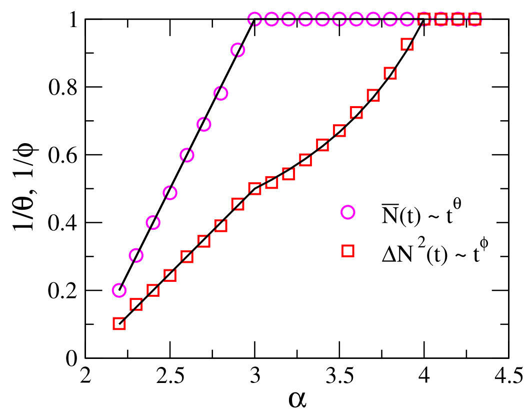

FIG. 3. Dynamic exponents associated with the average particle number θ and its quadratic fluctuations ϕ for distinct values of α. For $\alpha \geqslant 4$ the short-range values set up $\theta = \phi = 1$. For $2 < \alpha \leqslant 3$ one finds $\phi = 2\theta = 2/(\alpha - 2)$. For $3 \leqslant \alpha \leqslant 4$ one identifies an intermediate regime with $\theta = 1$ and $\phi = 5 - \alpha$.

lowered. Conversely, the population tends to cluster near the origin if $\alpha > 3$, leading to the same short-range $\theta = 1$ exponent. Figure 2(b) presents the log-log evolution in the fluctuations of the particle number. Note the same slope for $\alpha = 4$ and $\alpha = 4.5$. It is consistent with $\phi = 1$ for short-ranged branching. However, the dynamic exponent ϕ already starts to deviate from this value for $\alpha < 4$.

From the asymptotic slopes of the curves presented in Fig. 2, we obtained the dynamical critical exponents θ and ϕ for each α, as shown in Fig. 3. Note that the exponent $1/\theta$ monotonically grows for $\alpha < 3$ and converges to the short-range value $\theta = 1$ at $\alpha = 3$. This is so because the branching process tends to cluster the particles in a vicinity of the origin above this value of α, with the cluster front spreading ballistically. Creation and annihilation processes are balanced within the main cluster with the density of particles on it fluctuating around a constant value. As a consequence, the growth of the mean number of particles ends up being controlled by the ballistic evolution of the cluster front. For $\alpha < 3$, our data fits the empirical law $1/\theta = \alpha - 2$. The divergence of θ at $\alpha = 2$ signals the set up of exponential explosive growth of the population because annihilation becomes irrelevant at this extreme long-range regime where the average branching distance diverges.

For the dynamic exponent ϕ associated with the particle number fluctuations, we observe a similar behavior. However, the short-range value is reached only at $\alpha = 4$. This happens due the very nature of the underlying power-law processes, that allows for eventual long-distance jumps to occur, thus making second and higher moments larger than usual. Note also the occurrence of two distinct regimes $2 < \alpha \leqslant 3$ and $3 < \alpha \leqslant 4$. For $2 < \alpha < 3$, our data are consistent with the fluctuation exponent $\phi = 2\theta$. This means that the width of the particle number distribution becomes of the same order of the average number. Therefore, fluctuations are relevant in this regime, even in the long-time limit. On the other hand, $1 \leqslant \phi \leqslant 2$ for $3 \leqslant \alpha \leqslant 4$. Therefore, the width of the particle number distribution grows slower than its average in this regime, although faster than diffusively. This points to a

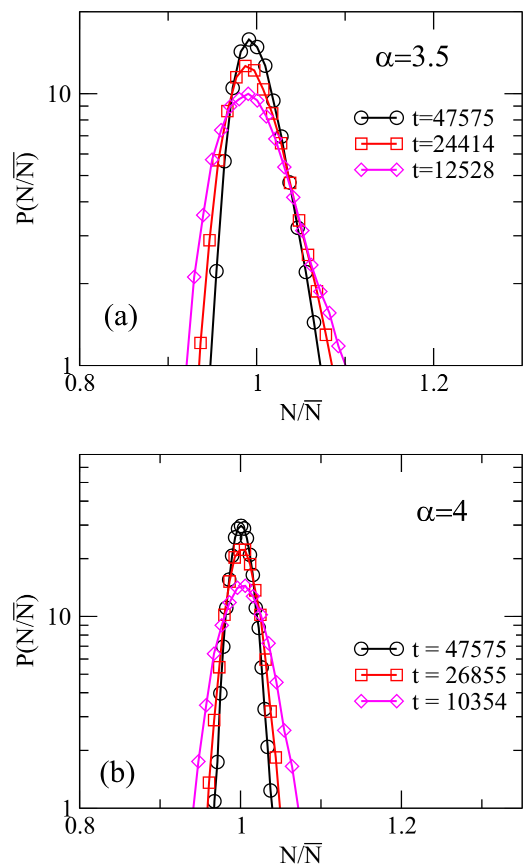

FIG. 4. Histograms for the particle number for $\alpha > 3$. In (a) we have $\alpha = 3.5$. There is a slow convergence to a Gaussian distribution. In (b) we have $\alpha = 4$ for which the convergence to Gaussian is faster.

weak violation of the central limit theorem in this regime. In this intermediate regime, our numerical data are well fitted by $\phi = 5 - \alpha$.

In order to have a deeper understanding of the dynamics in these distinct regimes, we present results concerning the histograms of the number of particles for different values of the range of the interaction, parameterized by α. In Fig. 4 we consider the cases $\alpha = 3.5$ and $\alpha = 4$. Here, the histograms were obtained from typically 4×10^4 samples. In Fig. 4(a) we observe that, as the time elapses, the probability distribution function (PDF) converges slowly to a normal distribution. For $\alpha = 4$ the PDF is Gaussian for all instants considered, as shown in Fig. 4(b). The short range of the interactions does not allow for large branching. Annihilation takes place and the convergence to a normal distribution occurs, as expected by the central limit theorem.

In Fig. 5(a) we present results for $\alpha = 2.3$ and $\alpha = 2.7$. We represent the probability $P(N/\overline{N})$ versus $N/\overline{N}$. Population N is calculated at $t = 446$ and $\overline{N}$ is averaged for 5×10^5 samples. The histograms are the same for other times and $\alpha < 3$ values, i.e., it represents the stationary distribution of the particle number in this regime. In Fig. 5(b) we use $\alpha = 3$ and consider three distinct instants t. Here, $\overline{N}$ is averaged over 10^4 samples. Notice that the distribution is also stationary in this regime, but presenting a profile distinct from that reported in Fig. 5(a). In both cases the distributions have a strongly non-Gaussian character.

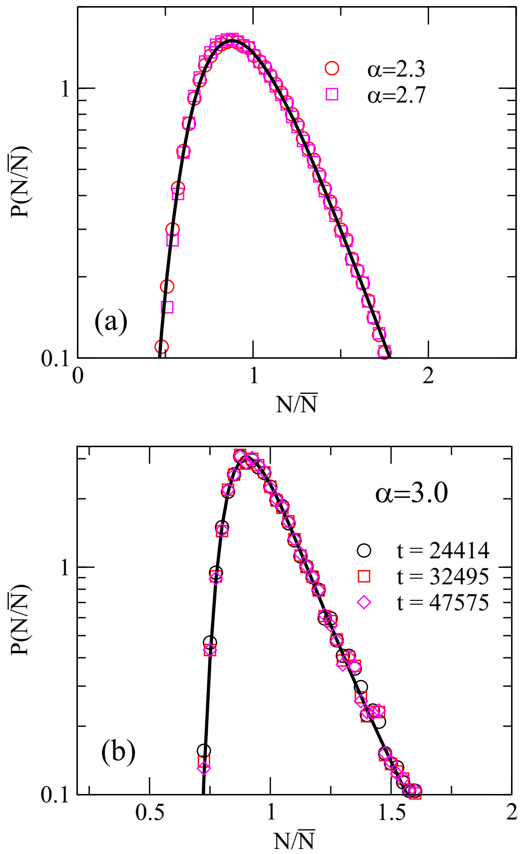

FIG. 5. In (a) we present the histogram for the number of particles N normalized over the mean number $N/\overline{N}$ for $\alpha = 2.3$ and $\alpha = 2.7$. These are fitted by a Gumbell distribution with $\sigma = 0.24$, $\xi = 0$, and $\mu = 0.88$ (solid line). In (b) we present $P(N/\overline{N})$ for $\alpha = 3.0$ at three different instants. The fit (solid line) represents a Frechet distribution with $\sigma = 0.12$, $\xi = 0.17$, and $\mu = 0.92$.

The above data were fitted by the extreme value stable Frechet and Gumbell distributions in the case of long range interaction $\alpha \leqslant 3$ (the regime with varying exponent θ). Gumbell and Frechet distributions are particular cases of the generalized extreme value (GED) distribution, which also includes the Weibull distribution [36]. The extreme value theorem states that these stable distributions describe the asymptotic behavior of normalized extreme values of an univariate independent sample. Frechet and Gumbell are obtained when we consider the maximum values of the variable. Conversely, a Weibull distribution is developed whenever one considers their minimum. The PDFs for these are given by

$$P(x) = \left(\frac{1}{\sigma}\right) t(x)^{\xi+1} e^{-t(x)} \tag{8}$$

with

$$t(x) = e^{-\frac{x-\mu}{\sigma}}, \quad \xi = 0 \tag{9}$$

$$t(x) = \left[1 + \xi\left(\frac{x-\mu}{\sigma}\right)\right]^{-1/\xi}, \quad \xi \neq 0. \tag{10}$$

The parameter ξ defines which one of the three distribution we are refereeing. The Gumbell distribution is obtained if $\xi = 0$, while $\xi > 0$ is for Frechet and $\xi < 0$ for Weibull. A Gumbell distribution fits the curves for $\alpha < 3$ with high accuracy with parameters $\sigma = 0.24$, $\xi = 0$, and $\mu = 0.88$. On the other hand, our data show the stationary property of the Frechet distribution in the threshold $\alpha = 3$ with $\sigma = 0.12$, $\xi = 0.17$, and $\mu = 0.92$. These results indicate that the dynamics is actually governed by the rare events of branching to sites far from the original seed.

It is important to mention that Gumbell distributions were also found to fit branching Brownian walkers, in which, after an exponential random time, the particle splits into n particles with a given probability. In [37] it was proved that the PDF of the maximum of branching Brownian motion converges to a Gumbell distribution, a conjecture previously stated in [38]. The largest extremes of independent and identically distributed random walks were also proved to converge to the Gumbell or the Frechet distributions [39]. Gumbell distributions were reported in random walks on fully connected lattices. In [40] the authors analyzed the time evolution in the number of sites visited within a given subset of the total number of sites. Whenever the walker visits any given site of this subset a value is recorded. When this recorded value equals the number of sites in the subset, the time value is dubbed total covering time and the fluctuations of this variable are distributed according a Gumbell distribution [40]. A recent experiment showed also a crossover from Frechet (at threshold) to Gumbell extreme value statistics in the intensities of a cw-pumped random fiber laser presenting underlying gain and Lévy processes [35]. The stimulated emission process responsible for the gain in lasers has a close analogy with the branching process while the Lévy trajectories of photons in random lasers gives the long-range character of the interactions. A loss process can be associated with the emission of photons when they reach the random laser borders. Our results indicate that extreme value distributions can emerge in general physical scenarios from the balance between gain and loss processes in systems with long-range interactions.

Before finishing, we will provide additional data in order to support the importance of long-distance branching extreme events to the systems dynamics. We start by reporting the time evolution of the spreading front $x_{\max}$, i.e., the distance from the seed position of the most distant particle at a given time. Data for some representative values of the branching exponent are shown in Fig. 6. While the spreading front evolves ballistically for $\alpha > 3$ with no major discontinuities, abrupt jumps resulting from long-distance branchings play a relevant role for $\alpha < 3$. In the time intervals between large jump events, the spreading front is mainly ballistic. However, these rare jump events give rise to an overall superballistic spreading and amplified fluctuations.

The spacial distribution of the particles at a given large time also unveils important aspects distinguishing the short- and long-range regimes. Far from the spreading front, the balance between branching and annihilation processes results in a statistically uniform particle distribution with the average occupation number of a given site being $\overline{n} = 1/2$ for both short- and long-ranged branching regimes. Fluctuations of the spreading front over distinct realizations produce a smooth crossover from the active region with $\overline{n} = 1/2$ to the inactive region with $\overline{n} = 0$. Depending on the branching regime,

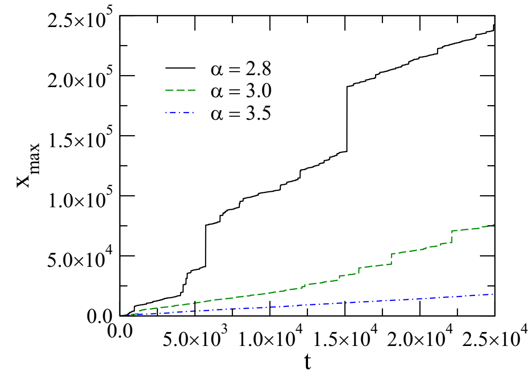

FIG. 6. Time evolution of the spreading front x_{max} measured as the distance from the seed position of the most distance particle at time t. Large jumps resulting from rare events of long-distance branchings become relevant for $\alpha < 3$, giving rise to a superballistic spreading and enhanced fluctuations.

quite distinct average occupation number distributions $\overline{n}(x)$ set up, as illustrated in Fig. 7. In the short-range regime, such crossover is exponential. Actually, the average occupation number distribution has a Fermi-Dirac form

$$\overline{n}(x) = \frac{n_0}{e^{\beta(x-x^*)}+1}, \tag{11}$$

where $n_0 = 1/2$, x^* is the distance to the origin on which the average occupation number decays to $n_0/2$, and β controls the width of the crossover region. The above Fermi-Dirac distribution fits accurately the simulation data for $\alpha = 4$ (solid line on the main frame of Fig. 7). We measured the distance in units of x^*, being left with a single fitting parameter βx^*. In this regime, the fitting parameter becomes larger when the distribution in measured at longer times, as expected, because the relative fluctuations become vanishing small in the Gaussian regime. The emergence of the Fermi-Dirac distribution is in line with the close analogy between reaction diffusion nonequilibrium problems and quantum fermionic systems [41,42] and can open a new direction towards future analytical derivations of the reported numerical distributions.

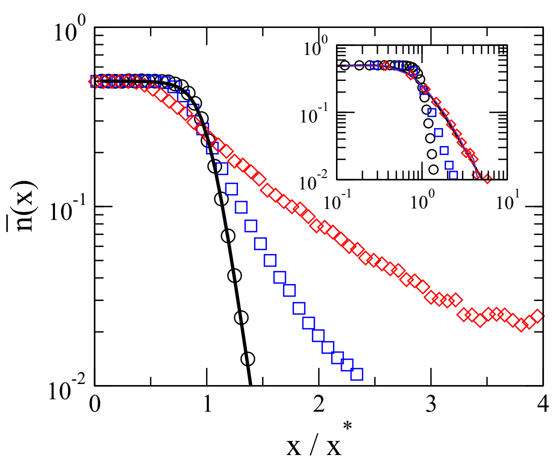

FIG. 7. Average occupation number distribution $\overline{n}(x)$ as a function of the normalized distance to the seed position x/x^*, where $\overline{n}(x^*) = n_0/2$. Data are for $\alpha = 4$ (circles), $\alpha = 3$ (squares), and $\alpha = 2.3$ (diamonds). Solid line is a fit to the Fermi-Dirac distribution given in Eq. (11). Inset: Double logarithmic plot of the same data. Solid line is a fit to the Fermi-Dirac distribution in the context of nonextensive statistics given in Eq. (12). Data were taken at $t = 100$ from 10^4 distinct realizations.

A very long crossover develops in the regime of long-range branchings. The average occupation number decays slowly for $x/x^* \gg 1$, typically as a power-law, as shown in the inset of Fig. 7 where the same data are plotted in double logarithmic scale. This feature is directly associated with the rare events of long-distance branchings that can populate regions at distances much larger than the average size of the active region. A generalization of the Fermi-Dirac distribution has been given in the literature in the context of nonextensive statistics [43–45] which has found applications in several physical systems presenting multifractality, long-time memory, and long-range interactions [46,47]. Although the exact form of the resulting Fermi-distribution is quite cumbersome and difficult to calculate, it assumes a simple and intuitive form within the so-called factorization approximation[48], being given by

$$\overline{n}(x) = \frac{n_0}{\{\exp_q[-\beta(x-x^*)]\}^{-1}+1}, \tag{12}$$

where

$$\exp_q(x) = [1+(1-q)x]^{1/(1-q)}, \tag{13}$$

for $1+(1-q)x > 0$, being zero otherwise. The above expression was used to fit the data for the average occupation number distribution at $\alpha = 2.3$, shown as the solid line in the inset of Fig. 7. Fitting parameters used were βx^* and q. βx^* is time independent in this regime because the particle number dispersion is of the same order as its average. The distribution decays as $1/(x/x^*)^{1/(q-1)}$. Our best fit for the $\alpha = 2.3$ distribution provided $q \simeq 1.46$. The above simple expression does not fit the entire particle number distribution in the intermediate regime of α values, a signal that relevant corrections to the factorization approximation are in order.

IV. SUMMARY AND CONCLUSIONS

In summary, we studied the dynamics of a branching and annihilating process of static particles that generate a single offspring and annihilate upon contact. The branching distance r was supposed to follow a Lévy power-law distribution, parametrized by the exponent α that governs the effective range of the branching process.

For $\alpha \geqslant 4$ the system is in the regime of very short ranged branching. The mean number of particles $\overline{N}(t)$ and its quadratic fluctuations grow linearly with time, as expected for branching to the close vicinity of the parental particle. The distribution of the number of particles N at a given time, determined from a large number of independent runs, quickly converge to a Gaussian.

For the intermediate regime of $3 < \alpha < 4$, the system still presents a linear growth in $\overline{N}(t)$ but the particle number quadratic fluctuations behave like $\Delta N^2(t) \propto t^{\phi}$ with $1 < \phi < 2$, which implies in a superdiffusive widening of the particle number distribution. Our data allowed us to propose the empirical relation $\phi = 5 - \alpha$. As the time evolves the distribution $P(N/\overline{N})$ slowly converges to a Gaussian.

For $2 < \alpha \leqslant 3$, both $\overline{N}$ and $\Delta N^2(t)$ obey power-law growths with dynamical exponents varying continuously with α. Our data are consistent with $\phi = 2\theta = 2/(\alpha - 2)$. In this regime, the width of the particle number distribution becomes of the same order as the own average particle number, thus signaling non-Gaussian asymptotic fluctuations. The PDFs $P(N/\overline{N})$ are best fitted by extreme value distributions, namely a Frechet distribution for the threshold value $\alpha = 3$ and a Gumbell distribution for $2 < \alpha < 3$, in close analogy with experimental findings in cw-pumped random fiber lasers experiments [35]. This result unveils the relevant role played by the events of extreme branching distances in this regime. Finally the dynamic exponents diverge for $\alpha \leqslant 2$, signalizing the explosive exponential population growth dominated by very long-ranged branching on which annihilation becomes irrelevant. The average occupation number distribution was shown to have a Fermi-Dirac aspect for short-range branchings, evolving to the corresponding one in the context of nonextensive statistics in the long-range regime.

The present work adds to the current literature supporting the emergence of extreme value statistic is dynamical systems with underlying Lévy processes. Due to the ubiquitous occurrence of Lévy distributions in nature [49–53], it would be valuable to have future investigations aiming to explore the possible emergence of extreme value distributions in general population dynamics models and optical systems with long-range interactions. It would also be interesting to have future analytical efforts aiming to derive the reported distributions exploring field theoretical and master equation approaches as well as the analogy between diffusion reaction problems and quantum fermionic model systems.

ACKNOWLEDGMENTS

This work was supported by CAPES (Coordenação de Aperfeiçoamento de Pessoal de Nível Superior), CNPq (Conselho Nacional de Desenvolvimento Científico e Tecnológico), FAPEAL (Fundação de Apoio à Pesquisa do Estado de Alagoas), and FACEPE (Fundação de Amparo à Ciência e Tecnologia do Estado de Pernambuco). M.L.L. acknowledges the hospitality of the Physics Department of Federal University of Pernambuco where this work has been partially developed with financial support from a partnership program CAPES/FACEPE (Grant No. APQ-0325-1.05/18).

[1] J. L. Cardy and U. C. Tauber, J. Stat. Phys. **90**, 1 (1998).
[2] M. Henkel and H. Hinrichsen, J. Phys. A: Math. Gen. **37**, R117 (2004).
[3] I. Jensen, J. Phys. A: Math Gen. **26**, 3921 (1993).
[4] D. Zhong and D. benAvraham, Phys. Lett. A **209**, 333 (1995).
[5] D. ben-Avraham, F. Leyvraz, and S. Redner, Phys. Rev. E **50**, 1843 (1994).
[6] E. V. Albano, Europhys. Lett. **34**, 97 (1996).
[7] L. H. Tang and G. S. Tian, Physica A **264**, 543 (1999).
[8] K. Mussawisade, J. E. Santos, and G. M. Schutz, J. Phys. A: Math Gen **31**, 4381 (1998).
[9] G. Szabo, Phys. Rev. E **62**, 7474 (2000).
[10] G. Odor, Phys. Rev. E **70**, 066122 (2004).
[11] F. Benitez and N. Wschebor, Phys. Rev. E **86**, 010104(R) (2012).
[12] E. V. Albano, M. Hoyuelos, and H. O. Martin, Physica A **239**, 531 (1997).
[13] J. Marro and R. Dickman, *Non-equilibrium Phase Transitions in Lattice Models* (Cambridge University Press, Cambridge, 1999).
[14] H. Hinrichsen, Adv. Phys. **49**, 815 (2000).
[15] F. Bagnoli, B. Chopard, M. Droz, and L. Frachebourg, J. Phys. A: Math. Gen. **25**, 1085 (1992).
[16] E. C. da Costa and F. R. Rusch, Physica A **451**, 565 (2016).
[17] H. Takayasu and A. Yu. Tretyakov, Phys. Rev. Lett. **68**, 3060 (1992).
[18] J. Cardy and U. C. Tauber, Phys. Rev. Lett. **77**, 4780 (1996).
[19] I. Jensen and R. Dickman, J. Stat. Phys. **71**, 89 (1993).
[20] I. Jensen, Phys. Rev. E **47**, R1 (1993).
[21] N. Inui, Phys. Lett. A **184**, 79 (1993).
[22] I. Jensen, Phys. Rev. E **50**, 3623 (1994).
[23] H. Taksyssu and N. Inui, J. Phys. A **25**, L585 (1992).
[24] S. Kwon and H. Park, Phys. Rev. E **52**, 5955 (1995).
[25] C. Argolo, Physica A **537**, 122731 (2020).
[26] H. Hinrichsen, J. Stat. Mech. (2007) P07006.
[27] H. K. Janssen, K. Oerding, F. van Wijland, and H. J. Hilhorst, Eur. Phys. J. B **7**, 137 (1999).
[28] D. Vernon and M. Howard, Phys. Rev. E **63**, 041116 (2001).
[29] T. Laise, P. Barros, C. Argolo, and M. L. Lyra, J. Stat. Mech. (2016) P113205.
[30] T. Laise, F. C. dos Anjos, C. Argolo, and M. L. Lyra, Physica A **505**, 648 (2018).
[31] K. B. Erickson, Ann. Prob. **1**, 926 (1973).
[32] A. Sudbury, Ann. Prob. **18**, 581 (1990).
[33] C. Neuhauser and A. Sudbury, Adv. Appl. Prob. **25**, 24 (1993).
[34] M. Bransom, W. D. Ding, and R. Durrett, Stoch. Proc. Appl. **37**, 1 (1991).
[35] B. C. Lima, P. I. R. Pincheira, E. P. Raposo, L. S. Menezes, C. B. de Araújo, A. S. L. Gomes, and R. Kashyap, Phys. Rev. A **96**, 013834 (2017).
[36] S. Coles, *An Introduction to Statistical Modeling of Extreme Values* (Springer-Verlag, London, 2001).
[37] L. P. Arguin, A. Bovier, and N. Kistler, Electron. J. Probab. **18**, 53 (2013).
[38] S. P. Lalley and T. Sellke, Ann. Probab. **15**, 1052 (1987).
[39] T. Mikosch and J. Yslas, Adv. Appl. Prob. **52**, 213 (2020).
[40] L. Turban, J. Phys. A: Math. Gen. **48**, 445001 (2015).
[41] F. C. Alcaraz, M. Droz, M. Henkel, and V. Rittenberg, Ann. Phys. (NY) **230**, 250 (1994).
[42] M. Henkel, E. Orlindini, and J. Santos, Ann. Phys. (NY) **259**, 163 (1997).
[43] A. K. Rajagopal, R. S. Mendes, and E. K. Lenzi, Phys. Rev. Lett. **80**, 3907 (1998).

[44] E. K. Lenzi, R. S. Mendes, and A. K. Rajagopal, Phys. Rev. E **59**, 1398 (1999).
[45] H. Hasegawa, Phys. Rev. E **80**, 011126 (2009).
[46] C. Tsallis, J. Stat. Phys. **52**, 479 (1988).
[47] C. Tsallis, Physica D **193**, 3 (2004).
[48] F. Büyükilic, D. Demirhan, and A. Gülec, Phys. Lett. A **197**, 209 (1995).
[49] C. Tsallis, S. V. F. Levy, A. M. C. Souza, and R. Maynard, Phys. Rev. Lett. **75**, 3589 (1995).
[50] M. F. Shlesinger, J. Klafter, and G. Zumofen, Am. J. Phys. **67**, 1253 (1999).
[51] G. M. Viswanathan, F. Bartumeus, S. V. Buldyrev, J. Catalan, U. L. Fulco, S. Havlin, M. G. E. da Luz, M. L. Lyra, E. P. Raposo, and H. E. Stanley, Physica A **314**, 208 (2002).
[52] G. M. Viswanathan, U. L. Fulco, M. L. Lyra, and M. Serva, Physica A **329**, 273 (2003).
[53] F. Bartumeus, M. G. E. da Luz, G. M. Viswanathan, and J. Catalan, Ecology **86**, 3078 (2005).